Anomalous Spin-Charge Separation in a Driven Hubbard System

Hongmin Gao,[1,*] Jonathan R. Coulthard,[1] Dieter Jaksch,[1,2] and Jordi Mur-Petit[1,†]
[1]Clarendon Laboratory, University of Oxford, Parks Road, Oxford OX1 3PU, United Kingdom
[2]Centre for Quantum Technologies, National University of Singapore, 3 Science Drive 2, 117543 Singapore

(Received 22 May 2020; accepted 5 October 2020; published 2 November 2020)

Spin-charge separation (SCS) is a striking manifestation of strong correlations in low-dimensional quantum systems, whereby a fermion splits into separate spin and charge excitations that travel at different speeds. Here, we demonstrate that periodic driving enables control over SCS in a Hubbard system near half filling. In one dimension, we predict analytically an exotic regime where charge travels slower than spin and can even become "frozen," in agreement with numerical calculations. In two dimensions, the driving slows both charge and spin and leads to complex interferences between single-particle and pair-hopping processes.

DOI: 10.1103/PhysRevLett.125.195301

Introduction.—Strongly correlated quantum systems exhibit a plethora of interesting phenomena, such as high-T_c superconductivity [1] or the fractional quantum Hall effect [2], underpinned by a competition between different interactions and orderings of different degrees of freedom [3]. An example of this is the delicate interplay between magnetic and charge correlations in the ground state of lightly doped high-T_c superconductors [4–7] that appears very sensitive to coherent processes beyond nearest neighbors [8–14]. A striking manifestation of strong fermionic correlations is spin-charge separation (SCS) [15–18], where the elementary excitations of the system are solitonlike spin and charge (or density) excitations, of which the physical fermion appears as a composite [19–22]. In one-dimensional (1D) systems, SCS is predicted to occur at low energies in Luttinger liquids [15]. Numerical simulations of the 1D Hubbard model also demonstrated SCS [23] in a regime beyond low energy that is relevant to cold-atom implementations of the model [24]. More recently, Ref. [25] studied the charge and spin transport properties of the 1D Hubbard model at finite temperature using a hydrodynamic approach. A typical signature of the distinct nature of spin and charge excitations in these systems is their very different propagation velocities. For instance, in the t-J model, spin excitations travel through the lattice at speed $u_s \sim Ja$, while the charge excitations move at speed $u_c \sim ta$ [26]; here a is the lattice constant, t is the hopping energy, and $J \ll t$ is the second-order exchange energy [see Eq. (1) below]. A recent cold-atom experiment confirmed these by tracking the real-time dynamics [27]. SCS has also been observed in condensed-matter setups through measurements of the dispersions of the excitations [16–18].

In contrast to the situation in 1D, the existence of SCS in the two-dimensional (2D) Hubbard and t-J models is an open question, owing partly to the lack of 2D analytical methods and partly to the limitations of current numerical methods [19–21,28–30]. There is evidence that the t-J model at low fermion density is consistent with the description of a Fermi liquid [31], whereas at higher fillings it shows SCS with a speed of charge excitations larger than that of spin excitations [19].

In this Letter, we demonstrate control over SCS via periodic driving of a strongly repulsive Hubbard model near half filling in 1D and 2D. It is known that such a system is well described by a static t-J-α model [32–37], where double occupancies are forbidden by the strong on-site repulsion in the underlying Hubbard system. Compared to the standard t-J model, the t-J-α model also includes three-site processes that play, as we show here, an important role in the dynamics. In 1D, we use matrix product state methods to look at the evolution of small localized spin and charge excitations of the effective t-J-α chain from its ground state. We identify an exotic regime, where the spin excitation speed exceeds that of the charge excitation. Interestingly, for some driving strengths before the occurrence of phase separation [38,39], we observe a ballistic propagation of spin excitations accompanied by "freezing" of charge excitations, a phenomenon that cannot be explained by dynamic localization [40] or self-localization by the phase-string effect [41]. Moreover, the novel freezing behavior is not seen in the standard t-J chain, where the charge excitations remain mobile until phase separation occurs. In 2D, we perform exact diagonalization calculations on a square lattice with a spin-dependent checkerboard potential, which creates initially imbalanced density and spin profiles from the ground state. After removing the potential, these imbalances oscillate in time, with different characteristic frequencies, which we show can be controlled by the driving. These predictions can be readily tested with available experimental techniques in the field of ultracold atoms [42–49], which will provide novel

information on the interplay between density and spin degrees of freedom in strongly interacting Hubbard systems [8–14] and could assist investigations on SCS in hitherto poorly understood regimes, such as in 2D models and high-energy excitations of 1D strongly interacting systems.

The t-J-α model.—We consider a system of strongly repulsive spin-1/2 fermions on a lattice. We describe this system with a Hubbard model $\hat{H}_{\rm Hub} = \hat{H}_{\rm hop}(t_0) + U\sum_i \hat{n}_{i\uparrow}\hat{n}_{i\downarrow}$. Here $\hat{H}_{\rm hop}(t_0) = -t_0\sum_{\langle ij\rangle\sigma}(\hat{c}^\dagger_{i\sigma}\hat{c}_{j\sigma} + \text{H.c.})$ describes the hopping between nearest-neighbor (NN) sites $\langle ij\rangle$ of a spin-σ fermion ($\sigma = \uparrow, \downarrow$), created at site i by $\hat{c}^\dagger_{i\sigma}$; t_0 is the fermion hopping amplitude between NN sites, and $\hat{n}_{i\sigma} = \hat{c}^\dagger_{i\sigma}\hat{c}_{i\sigma}$ is the density at site i of spin-σ fermions. Finally, the on-site repulsion energy $U \gg t$ prevents double occupation of a single site. We subject the system to a periodic driving of the form $\hat{H}_{\rm drive}(\tau) = \cos(\Omega\tau)\sum_i \boldsymbol{V}\cdot\boldsymbol{r}_i\hat{n}_i$, with frequency Ω and amplitude in the $x-y$ lattice plane $\boldsymbol{V} = (V_x, V_y)$; $\hat{n}_i = \hat{n}_{i\uparrow} + \hat{n}_{i\downarrow}$.

Under the condition $t_0 \ll \{U, \Omega, |U + m\Omega| \ \forall \ m \in \mathbb{Z}\}$, i.e., the driving is off resonant and fast compared to hopping, the dynamics of the driven system is described by an effective static t-J-α model (see Fig. 1)

$$\hat{H}_{tJ\alpha} = \mathcal{P}_0\{\hat{H}_{\rm hop}(t) + \hat{H}_{\rm ex}(J) + \hat{H}_{\rm pair}(\{\alpha_{ijk}\})\}\mathcal{P}_0, \quad (1)$$

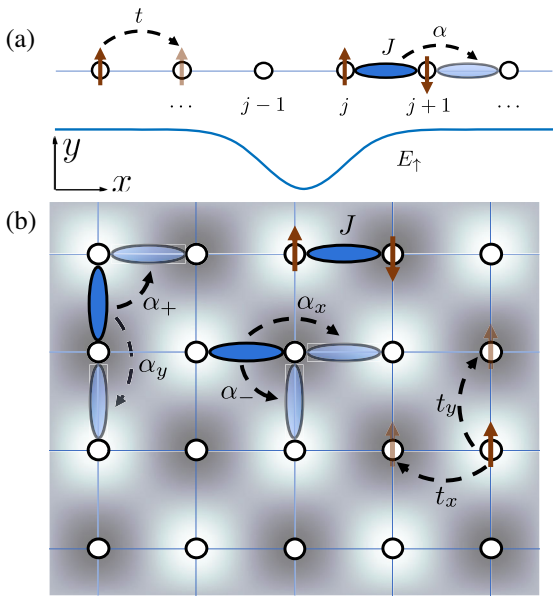

FIG. 1. (a) One-dimensional t-J-α chain. Spin-1/2 fermions (arrows) can hop between neighboring sites (circles) with hopping amplitude t. Nearest-neighbor singlet pairs (blue ellipse) are bound by a superexchange energy J and can hop from one bond to a neighboring bond with pair-hopping amplitude α. The bottom blue line illustrates the spin-dependent potential $\hat{V}_{\rm 1D}$, felt only by the ↑ species. (b) Two-dimensional t-J-α model. Generally, the single fermion ($t_{x,y}$), and singlet-pair-hopping ($\alpha_{x,y,\pm}$) amplitudes are anisotropic. The background shading indicates a staggered spin-dependent potential superimposed on the lattice.

with its parameters dependent on Ω and $\boldsymbol{V}$. The effective model (1) can be derived using a generalized Schrieffer-Wolff transformation [32,33] or a perturbative expansion in the Floquet basis [34–37]; see details in the Supplemental Material [50]. Here, the operator $\mathcal{P}_0 = \prod_i(1 - \hat{n}_{i\uparrow}\hat{n}_{i\downarrow})$ projects out states with double occupancies, $\hat{H}_{\rm ex}(J) = -J\sum_{\langle ij\rangle}\hat{b}^\dagger_{ij}\hat{b}_{ij}$ is the superexchange contribution, by which NN opposite spins switch their positions, $\hat{b}^\dagger_{ij} = (\hat{c}^\dagger_{i\uparrow}\hat{c}^\dagger_{j\downarrow} - \hat{c}^\dagger_{i\downarrow}\hat{c}^\dagger_{j\uparrow})/\sqrt{2}$ creates a spin-singlet pair straddling NN sites i and j, and $\hat{H}_{\rm pair}(\{\alpha_{ijk}\}) = -\sum_{\langle ijk\rangle}^{i\neq k}\alpha_{ijk}\hat{b}^\dagger_{ij}\hat{b}_{jk} + \text{H.c.}$ describes processes by which a singlet pair hops between nearby lattice bonds $\langle jk\rangle \to \langle ij\rangle$, see Fig. 1.

Anomalous SCS in one dimension.—We consider first the case of a 1D chain with open boundary conditions, shaken with dimensionless amplitude $K = |V|/\Omega$ along its length L. Equations (4) and (5) below provide the parameters of the corresponding effective t-J-α model: $t = t_0\mathcal{J}_0(K)$, $J = 4t_0^2\sum_m \mathcal{J}_m^2(K)/(U + m\Omega)$, and $\alpha = 2t_0^2\sum_m \mathcal{J}_m(K)\mathcal{J}_{-m}(K)/(U + m\Omega)$. Here $\mathcal{J}_m(K)$ is the mth-order Bessel function of the first kind. In the limit $U \gg \Omega$, these expressions reduce to $J \approx J_0 \equiv 4t_0^2/U$ and $\alpha \approx J_0\mathcal{J}_0(2K)/2$.

To study the dynamics of spin and charge degrees of freedom in this system, following Ref. [23] we add a weak spin-dependent potential, $\hat{V}_{\rm 1D} = -E_\uparrow\sum_j \exp[-(j - L/2)^2/2s^2]\hat{n}_{j,\uparrow}$, in order to create a localized spin-polarized density excitation in the center of the lattice, see Fig. 1(a). We then analyze the dynamics of the spin and density degrees of freedom upon removal of $\hat{V}_{\rm 1D}$, looking for signatures of SCS.

To start, we compute the ground state of the t-J-α model corresponding to the Hubbard model with given driving strength K, frequency Ω, and spin-dependent potential strength $E_\uparrow$ using the density matrix renormalization group (DMRG) algorithm [56,57]. At time $\tau = 0$, the spin-dependent potential is switched off (while still undergoing periodic driving) and we compute the system's evolution under the effective t-J-α model using the time evolving block decimation (TEBD) algorithm [57,58]. Note that all our simulations are performed with the t-J-α model, rather than the driven Hubbard model. The validity of the t-J-α model as a description of the Hubbard model driven with $\hat{H}_{\rm drive}$ is established in Ref. [37]. Reference [36] presents further evidence that driving-induced Floquet heating in these models remains low for driving durations $\lesssim 100/t_0$. For both DMRG and TEBD calculations, we employ the Tensor Network Theory library [59].

Our numerical results are summarized in Fig. 2, which shows the time evolution of the local spin $s^z_j = \langle\hat{s}^z_j\rangle$ and density $n_j = \langle\hat{n}_j\rangle$, with $\langle\hat{O}\rangle = \langle\psi(\tau)|\hat{O}|\psi(\tau)\rangle$, $|\psi(\tau)\rangle$ being the state of the system at time τ. The leftmost column shows the undriven system, $K = 0$. The initial spin-polarized charge excitation is localized in the center of the lattice. After $\hat{V}_{1D}$ is removed at $\tau = 0$, the excitation separates into

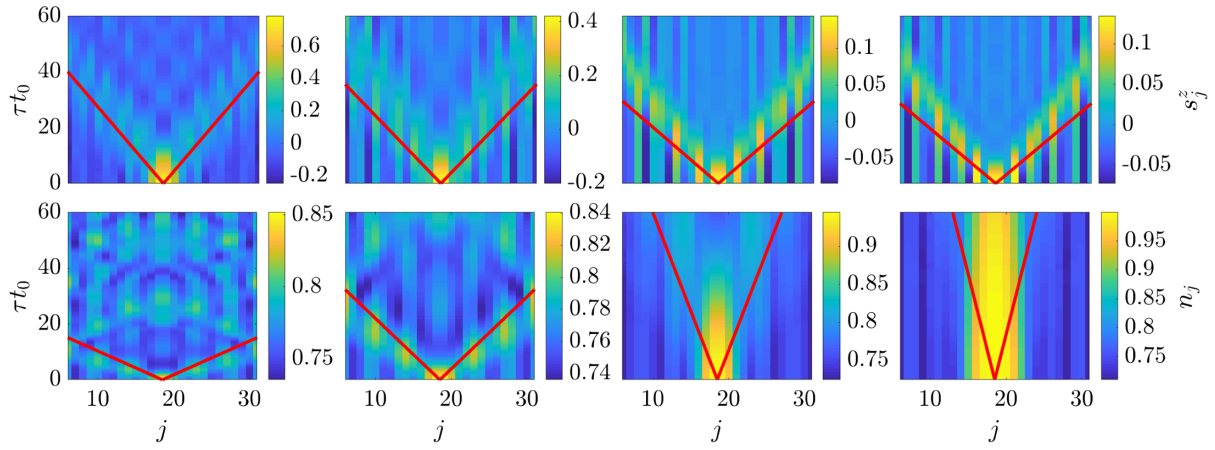

FIG. 2. Dynamics of local spin, $\langle \hat{s}_j^z \rangle$ (top row), and density, $\langle \hat{n}_j \rangle$ (bottom row), for the 1D t-J-α model as a function of position, j, and time, τ, after the removal of the spin-dependent potential. From left to right, the driving strengths used are $K = 0$, 1.5, 2.0, and 2.1, respectively. Note the different colorbar scales for each panel. The straight red lines are ballistic propagation velocity predictions from mean-field spin-charge separation (MF-SCS) theory (Supplemental Material [50]). Simulation parameters are: $U = 21t_0$ (such that $J_0 = 0.19t_0$), $\Omega = 6t_0$, $E_\uparrow = 0.5 \times \max\{|t|, J, |\alpha|\}$ and $s = 2$. The lattice contains $L = 36$ sites, of which the central 26 are shown. The total number of fermions is 28 (14 spin-$\uparrow$ + 14 spin-$\downarrow$), resulting in an average filling of $n = 7/9$.

a spin excitation that propagates at a speed $u_s \approx Ja$ and a charge excitation that propagates at a higher speed $u_c \approx ta$. As the driving strength increases, Eqs. (4) and (5) predict that t is suppressed while J remains approximately constant. In agreement with this prediction, our numerics shows that spin dynamics remain relatively unchanged, while the density dynamics changes drastically. For $K \gtrsim 2$ (third and fourth columns in Fig. 2), we reach an exotic regime where spin excitations travel *faster* than charge excitations. This inversion of the usual SCS scenario appears in its extreme version for $K \gtrsim 2.1$, when the charge excitation remains stationary ("freezes") at the lattice center, despite the fact that $t \neq 0$ (in fact, $t \approx J$). This anomalous SCS is a robust phenomenon, as the inversion of the relative velocities of charge and spin occurs for a broad range of parameters $(t_0, J_0, \Omega, \ldots)$.

The fact that the freezing happens before $t = 0$ (which occurs at $K \approx 2.404$) distinguishes this phenomenon from dynamic localization [40]. We also checked that it is not related to phase separation [38,39] by computing the inverse compressibility, which is nonvanishing for $2.1 \lesssim K \lesssim 2.2$. Charge in t-J models has also been shown to localize due to the phase-string effect [41], however, this effect only occurs in spatial dimensions higher than 1, which excludes self-localization as an explanation for the freezing observed here. Instead, we rationalize that it stems from the interplay between the direct (t) and spin-correlated (α) hopping of fermions. This is supported by the fact that, if $\alpha = 0$, the charge dynamics is frozen only at stronger driving, $K \gtrsim 2.3$, when phase separation occurs [39].

We compare the numerical results with analytical calculations using a mean-field spin-charge separation (MF-SCS) theory based on Ref. [51]. We find that pair-hopping (α) processes affect the charge u_c and spin u_s excitation velocities already at this mean-field (MF) level. Specifically, we find

$$u_c = u_c^{t\text{-}J} + 4\alpha n \chi^2 \sin[2\pi(1-n)], \tag{2}$$

$$u_s = u_s^{t\text{-}J} + 4\alpha n \phi \chi, \tag{3}$$

where $u_c^{t\text{-}J} = -4t\chi \sin[\pi(1-n)]$ and $u_s^{t\text{-}J} = J(n^2 - \phi^2)(1-2\chi) - 4t\phi$ are, respectively, the MF charge and spin velocities of the t-J model [51], n is the filling fraction ($n = 1$ for half filling), and $\chi(\phi)$ is the MF value of the fermions describing neighboring-site spin (charge) coherence; see Eqs. (S.20) and (S.21) in the Supplemental Material [50]. At weak driving, $|\alpha| \ll t$, and u_c is close to that for the standard t-J model [51]. At larger drivings ($K > 1.2$), the pair-hopping (α) terms gain in importance and affect the dispersions of separated spin and charge degrees of freedom [see Eqs. (S.26) and (S.27) in [50]], such that u_c is lower than in the t-J model [see Fig. S.2 in [50]]. These predictions are in good agreement with our numerics, as shown by the solid lines in the lower panels of Fig. 2. We note that our MF-SCS theory predicts freezing of charge excitations even though at a larger value of K than the numerics (see Fig. 2, bottom right panel).

Regarding the spin excitation velocity u_s, our MF-SCS theory predicts with accuracy its value at half filling [50]. For the t-J model, it is known from exact calculations that u_s depends very weakly on n near half filling [26]. We thus follow Ref. [51] and compare our MF-SCS prediction for u_s at half filling with our numerical results at $n = 7/9$ in the top panels of Fig. 2. We observe a fair agreement given the considerable assumptions of the MF treatment. We note that, similar to what happens in the t-J model, a fully self-consistent MF treatment overestimates the contribution of

single-particle hopping to u_s away from half filling, leading to a strong n dependence; see Fig. S.1 in the Supplemental Material [50].

Anisotropic transport and SCS in two dimensions.—We consider next the SCS scenario on a square lattice under sinusoidal time-periodic driving. For this case, the effective single-particle hopping amplitudes between NN sites $\langle ij\rangle$ separated along the $\eta = \{x, y\}$ directions are

$$t_\eta = t_0 \mathcal{J}_0(K_\eta), \tag{4}$$

where $K_\eta = |V_\eta|/\Omega$. Superexchange processes have parameters $J_\eta = 4t_0^2 \sum_m \mathcal{J}_m^2(K_\eta)/(U + m\Omega)$ for NN sites separated along $\eta = \{x, y\}$. Finally, pair-hopping amplitudes α_{ijk} become anisotropic as well, with generally four different values, namely,

$$\alpha_\eta = 2t_0^2 \sum_m \frac{\mathcal{J}_m(K_\eta)\mathcal{J}_{-m}(K_\eta)}{U + m\Omega}, \qquad \mathbf{r}_i - \mathbf{r}_k \propto \boldsymbol{\eta} = \boldsymbol{x}, \boldsymbol{y},$$
$$\alpha_\pm = 2t_0^2 \sum_m \frac{\mathcal{J}_m(K_x)\mathcal{J}_{\pm m}(K_y)}{U + m\Omega}, \qquad \mathbf{r}_i - \mathbf{r}_k \propto \boldsymbol{e}_\pm, \tag{5}$$

where $\boldsymbol{e}_\pm = (\boldsymbol{x} \pm \boldsymbol{y})/\sqrt{2}$.

We study the system driven with dimensionless amplitudes $K_x = -K_y = K$, i.e., $\boldsymbol{V} \propto \boldsymbol{e}_-$. In this case, the single-particle hopping amplitudes along the x and y directions are suppressed equally, $t_x = t_y \equiv t = t_0 \mathcal{J}_0(K)$ [Eq. (4)], while the superexchange parameter is equal across all NN bonds, $J_x = J_x \equiv J$. According to Eq. (5), the singlet-pair-hopping amplitudes are anisotropic and larger along $\boldsymbol{e}_+$: $\alpha_x = \alpha_y = \alpha_- \neq \alpha_+$. For instance, in the limit $U \gg \Omega$, one has $\alpha_- \approx J\mathcal{J}_0(2K)/2$ and $\alpha_+ \approx J/2 > |\alpha_-|$. This anisotropy arises because, under the driving, a singlet pair's potential energy changes by the same amount after hopping along the $x/y/\boldsymbol{e}_-$ direction, but it does not change for hopping along $\boldsymbol{e}_+$.

To analyze the dynamics of this system with reduced finite-size and boundary effects on our results from a potentially fast-spreading localized perturbation, we impose periodic boundary conditions and set up the initial state as the ground state of the t-J-α model in a weak spin-dependent potential with a checkerboard pattern, $\hat{V}_{2D} = -E_\uparrow^{2D} \sum_{j_x, j_y} (-1)^{j_x + j_y} n_{j\uparrow}$, where $j = (j_x, j_y)$ labels the rows and columns of the 2D lattice and $E_\uparrow^{2D}$ is the strength of the potential. We remove $\hat{V}_{2D}$ at time $\tau = 0$, and we use exact diagonalization to fully describe the quick growth of entanglement in the quenched system [57]. To monitor the spin and density dynamics, we compute density and spin imbalances defined as [60–63]

$$I_O(\tau) = \sum_{j_x, j_y} (-1)^{j_x + j_y} \langle \hat{O}_j(\tau)\rangle, \qquad O = n, s. \tag{6}$$

We see in Fig. 3 that both I_n and I_s show persistent oscillations, corresponding to spin and charge excitations

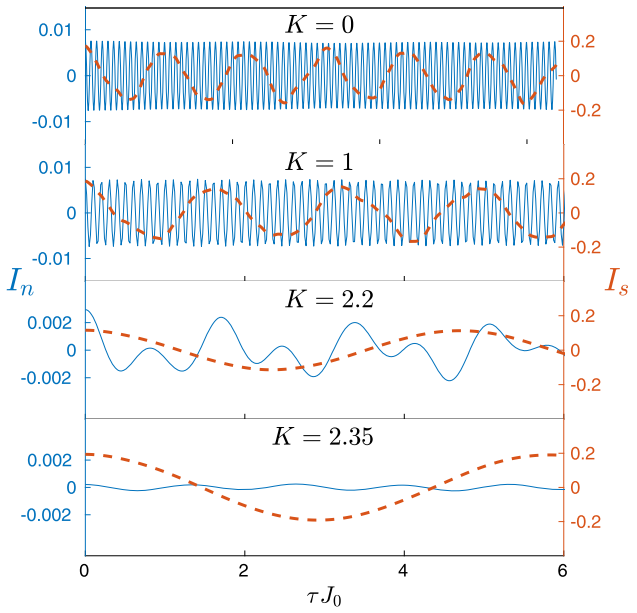

FIG. 3. Density (blue solid line, left axis) and spin (red dashed line, right axis) imbalance as a function of time for different driving strengths as indicated. The system is a diagonal stripe covering 12 sites of a square lattice perpendicular to the driving direction, with five spin-↑ and five spin-↓ fermions (Supplemental Material [50]). Simulation parameters are $U = 50t_0$ (such that $J_0 = 0.08t_0$), $\Omega = 14t_0$, and $E_\uparrow^{2D} \approx 0.05 \max\{|t|, J, |\alpha_\pm|\}$. Note the change of left y-axis limits in the lower two panels.

moving coherently between neighboring sites. Similar to the 1D case, for weak driving, $K \lesssim 1$ (top two panels in Fig. 3), the density dynamics is significantly faster than the spin dynamics. Strong driving $K > 2$ slows down the density dynamics much more compared to spin dynamics (lower panels in Fig. 3). In our simulations, $E_\uparrow^{2D}$ is kept as a constant fraction of the dominant energy scale of the t-J-α model. Thus, the reduction in the amplitude of I_n oscillations with increasing K is due to the t-J-α model becoming "stiffer" to the perturbation potential. On the other hand, the oscillation frequencies are practically unaffected by $E_\uparrow^{2D}$ and depend only on K [50]. This suggests that the changes in the spin and charge oscillation frequencies observed in Fig. 3 stem from the changing character of the excitations of the t-J-α model itself as its parameters are tuned with K.

While strong driving $K > 2$ leads to a slowing down of density dynamics, unlike the situation in 1D, we do not observe the density excitations becoming slower than the spin excitations, i.e., an inversion of the usual SCS relative speeds. In particular, it is not possible to reach the freezing limit in 2D. This appears to be due to an interplay between direct and spin-correlated hoppings. This interplay underpins, e.g., the complex I_n evolution observed for $K = 2.2$ in Fig. 3. To understand this, we note that $\alpha_+(K) \approx t(K)$ [37] for $K \approx 2.2$, which leads to an interference between hopping events to first and second neighbors

(Supplemental Material [50]). Numerical simulations of high-energy excitations in a lattice at low filling [37], where the dynamics is effectively described in terms of singlet pairs, also support the importance of pair-hopping terms in retaining a nonzero particle transport in 2D systems when $|t(K)| < J(K)$. These observations are in line with recent numerical findings pointing to the relevance of next-to-nearest-neighbor hopping amplitudes (t') to establish the ground-state charge and spin orderings of the Hubbard model near half filling [8–14].

Finally, it is worth noting the relevance of the driving directionality: had we chosen to drive along the x axis as in Ref. [64], t_x would be renormalized but $t_y = t_0 \gg \{J, |\alpha_{x,y,\pm}|\}$, and single-particle hopping would dominate the dynamics, as shown in Ref. [37].

In summary, we have demonstrated that periodic driving allows one to control density (or charge) transport in low-dimensional strongly correlated quantum systems and to enhance the competition between direct particle transport and spin-correlated pair-hopping processes. In particular, we showed that, in the 1D t-J-α model, the relative propagation speeds of the spin and charge excitations can be reversed into an exotic regime in which spin excitations travel faster than charge excitations. Moreover, we observed a regime of density freezing for moderately strong driving strengths, accessible by quasiadiabatic ramping of the driving [37]. In a 2D lattice, we established that driving can lead to a severe reduction in the propagation frequencies of both spin and charge excitations, reaching a regime where coherent processes involving next-to-nearest neighbors have an enhanced impact on single-particle transport. We expect these findings will open new routes to exploring unusual regimes of particle and spin transport and the interplay between magnetic and superconducting correlations, in equilibrium [8–14,65,66] and out-of-equilibrium [36,39,67–74] strongly correlated systems.

Our ideas can be implemented with existing cold-atom experimental technology [42–49]. This brings in the interesting possibility of tuning the effective dimensionality of the system, thus enabling one to explore in a controlled manner the role of dimensionality and anisotropy in charge and spin transport in Hubbard systems.

We would like to thank T. Esslinger, F. Görg, M. Messer, R. A. Molina, and S. Parameswaran for useful discussions. This work has been supported by EPSRC Grants No. EP/P01058X/1, No. EP/P009565/1, and No. EP/K038311/1, the Networked Quantum Information Technologies Hub (NQIT) of the UK National Quantum Technology Programme (EP/M013243/1), and by the European Research Council under the European Union's Seventh Framework Programme (FP7/2007-2013)/ERC Grant Agreement No. 319286 (Q-MAC). We acknowledge the use of the University of Oxford Advanced Research Computing (ARC) facility in carrying out this work. D. J. partially carried out this work while visiting the Institute for Mathematical Sciences, National University of Singapore.

H. C. and J. R. C. contributed equally to this work.

*hongmin.gao@physics.ox.ac.uk
†jordi.murpetit@physics.ox.ac.uk

[1] E. Fradkin, S. A. Kivelson, and J. M. Tranquada, Colloquium: Theory of intertwined orders in high temperature superconductors, Rev. Mod. Phys. **87**, 457 (2015).
[2] H. L. Stormer, D. C. Tsui, and A. C. Gossard, The fractional quantum Hall effect, Rev. Mod. Phys. **71**, S298 (1999).
[3] E. Dagotto, Complexity in strongly correlated electronic systems, Science **309**, 257 (2005).
[4] S. Gerber *et al.*, Three-dimensional charge density wave order in $YBa_2Cu_3O_{6.67}$ at high magnetic fields, Science **350**, 949 (2015).
[5] R. Comin and A. Damascelli, Resonant x-ray scattering studies of charge order in cuprates, Annu. Rev. Condens. Matter Phys. **7**, 369 (2016).
[6] E. H. Da Silva Neto, B. Yu, M. Minola, R. Sutarto, E. Schierle, F. Boschini, M. Zonno, M. Bluschke, J. Higgins, Y. Li, G. Yu, E. Weschke, F. He, M. Le Tacon, R. L. Greene, M. Greven, G. A. Sawatzky, B. Keimer, and A. Damascelli, Doping-dependent charge order correlations in electron-doped cuprates, Sci. Adv. **2**, e1600782 (2016).
[7] M. H. Julien, Magnetic fields make waves in cuprates, Science **350**, 914 (2015).
[8] B. X. Zheng, C. M. Chung, P. Corboz, G. Ehlers, M. P. Qin, R. M. Noack, H. Shi, S. R. White, S. Zhang, and G. K. L. Chan, Stripe order in the underdoped region of the two-dimensional Hubbard model, Science **358**, 1155 (2017).
[9] E. W. Huang, C. B. Mendl, S. Liu, S. Johnston, H. C. Jiang, B. Moritz, and T. P. Devereaux, Numerical evidence of fluctuating stripes in the normal state of high-T_c cuprate superconductors, Science **358**, 1161 (2017).
[10] J. F. Dodaro, H. C. Jiang, and S. A. Kivelson, Intertwined order in a frustrated four-leg t-J cylinder, Phys. Rev. B **95**, 155116 (2017).
[11] A. Nocera, N. D. Patel, E. Dagotto, and G. Alvarez, Signatures of pairing in the magnetic excitation spectrum of strongly correlated two-leg ladders, Phys. Rev. B **96**, 205120 (2017).
[12] E. W. Huang, C. B. Mendl, H. C. Jiang, B. Moritz, and T. P. Devereaux, Stripe order from the perspective of the Hubbard model, npj Quantum Mater. **3**, 22 (2018).
[13] H.-C. Jiang, Z.-Y. Weng, and S. A. Kivelson, Superconductivity in the doped t-J model: Results for four-leg cylinders, Phys. Rev. B **98**, 140505(R) (2018).
[14] H.-C. Jiang and T. P. Devereaux, Superconductivity in the doped Hubbard model and its interplay with next-nearest hopping t', Science **365**, 1424 (2019).
[15] F. D. M. Haldane, Luttinger liquid theory of one-dimensional quantum fluids. I. Properties of the Luttinger model and their extension to the general 1D interacting spinless Fermi gas, J. Phys. C **14**, 2585 (1981).

[16] O. M. Auslaender, H. Steinberg, A. Yacoby, Y. Tserkovnyak, B. I. Halperin, K. W. Baldwin, L. N. Pfeiffer, and K. W. West, Spin-charge separation and localization in one dimension, Science **308**, 88 (2005).

[17] Y. Jompol, C. J. B. Ford, J. P. Griffiths, I. Farrer, G. A. C. Jones, D. Anderson, D. A. Ritchie, T. W. Silk, and A. J. Schofield, Probing spin-charge separation in a Tomonaga-Luttinger liquid, Science **325**, 597 (2009).

[18] Y. Ma, H. C. Diaz, J. Avila, C. Chen, V. Kalappattil, R. Das, M.-H. Phan, T. Čadež, J. M. P. Carmelo, M. C. Asensio, and M. Batzill, Angle resolved photoemission spectroscopy reveals spin charge separation in metallic $MoSe_2$ grain boundary, Nat. Commun. **8**, 14231 (2017).

[19] W. O. Putikka, R. L. Glenister, R. R. P. Singh, and H. Tsunetsugu, Indications of Spin-Charge Separation in the Two-Dimensional *t-J* Model, Phys. Rev. Lett. **73**, 170 (1994).

[20] Y. C. Chen, A. Moreo, F. Ortolani, E. Dagotto, and T. K. Lee, Spin-charge separation in the two-dimensional Hubbard and *t-J* models at low electronic density, Phys. Rev. B **50**, 655 (1994).

[21] Z. Y. Weng, D. N. Sheng, and C. S. Ting, Spin-charge separation in the *t-J* model: Magnetic and transport anomalies, Phys. Rev. B **52**, 637 (1995).

[22] M. L. Kulić, Interplay of electron-phonon interaction and strong correlations: The possible way to high-temperature superconductivity, Phys. Rep. **338**, 1 (2000).

[23] C. Kollath, U. Schollwöck, and W. Zwerger, Spin-Charge Separation in Cold Fermi Gases: A Real Time Analysis, Phys. Rev. Lett. **95**, 176401 (2005).

[24] A. Recati, P. O. Fedichev, W. Zwerger, and P. Zoller, Spin-Charge Separation in Ultracold Quantum Gases, Phys. Rev. Lett. **90**, 020401 (2003).

[25] E. Ilievski and J. De Nardis, Ballistic transport in the one-dimensional Hubbard model: The hydrodynamic approach, Phys. Rev. B **96**, 081118(R) (2017).

[26] H. J. Schulz, Correlated fermions in one dimension, Int. J. Mod. Phys. B **05**, 57 (1991).

[27] J. Vijayan, P. Sompet, G. Salomon, J. Koepsell, S. Hirthe, A. Bohrdt, F. Grusdt, I. Bloch, and C. Gross, Time-resolved observation of spin-charge deconfinement in fermionic Hubbard chains, Science **367**, 186 (2020).

[28] A. S. Mishchenko, N. V. Prokof'ev, and B. V. Svistunov, Single-hole spectral function and spin-charge separation in the *t-J* model, Phys. Rev. B **64**, 033101 (2001).

[29] A. Läuchli and D. Poilblanc, Spin-Charge Separation in Two-Dimensional Frustrated Quantum Magnets, Phys. Rev. Lett. **92**, 236404 (2004).

[30] F. Trousselet, P. Horsch, A. M. Oleś, and W.-L. You, Hole propagation in the Kitaev-Heisenberg model: From quasiparticles in quantum Néel states to non-Fermi liquid in the Kitaev phase, Phys. Rev. B **90**, 024404 (2014).

[31] R. Eder and Y. Ohta, Spin and charge dynamics of the two-dimensional *t-J* model at intermediate electron densities: Absence of spin-charge separation, Phys. Rev. B **51**, 11683 (1995).

[32] A. Bermudez and D. Porras, Interaction-dependent photon-assisted tunneling in optical lattices: A quantum simulator of strongly-correlated electrons and dynamical gauge fields, New J. Phys. **17**, 103021 (2015).

[33] M. Bukov, M. Kolodrubetz, and A. Polkovnikov, Schrieffer-Wolff Transformation for Periodically Driven Systems: Strongly Correlated Systems with Artificial Gauge Fields, Phys. Rev. Lett. **116**, 125301 (2016).

[34] J. H. Mentink, K. Balzer, and M. Eckstein, Ultrafast and reversible control of the exchange interaction in Mott insulators, Nat. Commun. **6**, 6708 (2015).

[35] J. J. Mendoza-Arenas, F. J. Gómez-Ruiz, M. Eckstein, D. Jaksch, and S. R. Clark, Ultra-fast control of magnetic relaxation in a periodically driven Hubbard model, Ann. Phys. (Amsterdam) **529**, 1700024 (2017).

[36] J. R. Coulthard, S. R. Clark, S. Al-Assam, A. Cavalleri, and D. Jaksch, Enhancement of superexchange pairing in the periodically driven Hubbard model, Phys. Rev. B **96**, 085104 (2017).

[37] H. Gao, J. R. Coulthard, D. Jaksch, and J. Mur-Petit, Controlling magnetic correlations in a driven Hubbard system far from half-filling, Phys. Rev. A **101**, 053634 (2020).

[38] V. J. Emery, S. A. Kivelson, and H. Q. Lin, Phase Separation in the *t-J* Model, Phys. Rev. Lett. **64**, 475 (1990).

[39] J. R. Coulthard, S. R. Clark, and D. Jaksch, Ground-state phase diagram of the one-dimensional *t-J* model with pair hopping terms, Phys. Rev. B **98**, 035116 (2018).

[40] D. H. Dunlap and V. M. Kenkre, Dynamic localization of a charged particle moving under the influence of an electric field, Phys. Rev. B **34**, 3625 (1986).

[41] Z. Zhu, H.-C. Jiang, Y. Qi, C. Tian, and Z.-Y. Weng, Strong correlation induced charge localization in antiferromagnets, Sci. Rep. **3**, 2586 (2013).

[42] G. Jotzu, M. Messer, R. Desbuquois, M. Lebrat, T. Uehlinger, D. Greif, and T. Esslinger, Experimental realisation of the topological Haldane model with ultracold fermions, Nature (London) **515**, 237 (2014).

[43] R. Desbuquois, M. Messer, F. Görg, K. Sandholzer, G. Jotzu, and T. Esslinger, Controlling the Floquet state population and observing micromotion in a periodically driven two-body quantum system, Phys. Rev. A **96**, 053602 (2017).

[44] M. Messer, K. Sandholzer, F. Görg, J. Minguzzi, R. Desbuquois, and T. Esslinger, Floquet Dynamics in Driven Fermi-Hubbard Systems, Phys. Rev. Lett. **121**, 233603 (2018).

[45] M. F. Parsons, A. Mazurenko, C. S. Chiu, G. Ji, D. Greif, and M. Greiner, Site-resolved measurement of the spin-correlation function in the Fermi-Hubbard model, Science **353**, 1253 (2016).

[46] M. Boll, T. A. Hilker, G. Salomon, A. Omran, J. Nespolo, L. Pollet, I. Bloch, and C. Gross, Spin- and density-resolved microscopy of antiferromagnetic correlations in Fermi-Hubbard chains, Science **353**, 1257 (2016).

[47] L. W. Cheuk, M. A. Nichols, K. R. Lawrence, M. Okan, H. Zhang, E. Khatami, N. Trivedi, T. Paiva, M. Rigol, and M. W. Zwierlein, Observation of spatial charge and spin correlations in the 2D Fermi-Hubbard model, Science **353**, 1260 (2016).

[48] C. S. Chiu, G. Ji, A. Mazurenko, D. Greif, and M. Greiner, Quantum State Engineering of a Hubbard System with Ultracold Fermions, Phys. Rev. Lett. **120**, 243201 (2018).

[49] G. Salomon, J. Koepsell, J. Vijayan, T. A. Hilker, J. Nespolo, L. Pollet, I. Bloch, and C. Gross, Direct observation of incommensurate magnetism in Hubbard chains, Nature (London) **565**, 56 (2019).
[50] See Supplemental Material at http://link.aps.org/supplemental/10.1103/PhysRevLett.125.195301 for the derivation of the t-J-α Hamiltonian using Floquet theory, our MF-SCS calculation of spin and charge speeds, numerical details on the 2D simulations, and additional simulations illustrating the interference between t and α hoppings in 2D systems, which includes Refs. [26,36,40,51–55].
[51] S. Feng, Z. B. Su, and L. Yu, Fermion-spin transformation to implement the charge-spin separation, Phys. Rev. B **49**, 2368 (1994).
[52] J. H. Shirley, Solution of the Schrödinger equation with a Hamiltonian periodic in time, Phys. Rev. **138**, B979 (1965).
[53] M. Bukov, L. D'Alessio, and A. Polkovnikov, Universal high-frequency behavior of periodically driven systems: From dynamical stabilization to Floquet engineering, Adv. Phys. **64**, 139 (2015).
[54] A. Eckardt, Colloquium: Atomic quantum gases in periodically driven optical lattices, Rev. Mod. Phys. **89**, 011004 (2017).
[55] T. Giamarchi, *Quantum Physics in One Dimension* (Oxford University Press, Oxford, 2004).
[56] S. R. White, Density Matrix Formulation for Quantum Renormalization Groups, Phys. Rev. Lett. **69**, 2863 (1992).
[57] U. Schollwöck, The density-matrix renormalization group in the age of matrix product states, Ann. Phys. (Amsterdam) **326**, 96 (2011).
[58] G. Vidal, Efficient Simulation of One-Dimensional Quantum Many-Body Systems, Phys. Rev. Lett. **93**, 040502 (2004).
[59] S. Al-Assam, S. R. Clark, and D. Jaksch, The tensor network theory library, J. Stat. Mech. (2017) 093102.
[60] S. Trotzky, Y.-A. Chen, A. Flesch, I. P. McCulloch, U. Schollwöck, J. Eisert, and I. Bloch, Probing the relaxation towards equilibrium in an isolated strongly correlated one-dimensional Bose gas, Nat. Phys. **8**, 325 (2012).
[61] M. Schreiber, S. S. Hodgman, P. Bordia, H. P. Lüschen, M. H. Fischer, R. Vosk, E. Altman, U. Schneider, and I. Bloch, Observation of many-body localization of interacting fermions in a quasirandom optical lattice, Science **349**, 842 (2015).
[62] R. Landig, L. Hruby, N. Dogra, M. Landini, R. Mottl, T. Donner, and T. Esslinger, Quantum phases from competing short- and long-range interactions in an optical lattice, Nature (London) **532**, 476 (2016).
[63] P. Rosson, M. Kiffner, J. Mur-Petit, and D. Jaksch, Characterizing the phase diagram of finite-size dipolar Bose-Hubbard systems, Phys. Rev. A **101**, 013616 (2020).
[64] F. Görg, M. Messer, K. Sandholzer, G. Jotzu, R. Desbuquois, and T. Esslinger, Enhancement and sign change of magnetic correlations in a driven quantum many-body system, Nature (London) **553**, 481 (2018).
[65] P. Corboz, T. M. Rice, and M. Troyer, Competing States in the t-J Model: Uniform d-Wave State Versus Stripe State, Phys. Rev. Lett. **113**, 046402 (2014).
[66] M. Dolfi, B. Bauer, S. Keller, and M. Troyer, Pair correlations in doped Hubbard ladders, Phys. Rev. B **92**, 195139 (2015).
[67] R. Singla, G. Cotugno, S. Kaiser, M. Först, M. Mitrano, H. Y. Liu, A. Cartella, C. Manzoni, H. Okamoto, T. Hasegawa, S. R. Clark, D. Jaksch, and A. Cavalleri, THz-Frequency Modulation of the Hubbard U in an Organic Mott Insulator, Phys. Rev. Lett. **115**, 187401 (2015).
[68] M. Mitrano, A. Cantaluppi, D. Nicoletti, S. Kaiser, A. Perucchi, S. Lupi, P. Di Pietro, D. Pontiroli, M. Riccò, S. R. Clark, D. Jaksch, and A. Cavalleri, Possible light-induced superconductivity in K_3C_{60} at high temperature, Nature (London) **530**, 461 (2016).
[69] D. M. Kennes, E. Y. Wilner, D. R. Reichman, and A. J. Millis, Transient superconductivity from electronic squeezing of optically pumped phonons, Nat. Phys. **13**, 479 (2017).
[70] J. W. McIver, B. Schulte, F.-U. Stein, T. Matsuyama, G. Jotzu, G. Meier, and A. Cavalleri, Light-induced anomalous Hall effect in graphene, Nat. Phys. **16**, 38 (2020).
[71] J. Mur-Petit, A. Relaño, R. A. Molina, and D. Jaksch, Revealing missing charges with generalised quantum fluctuation relations, Nat. Commun. **9**, 2006 (2018).
[72] M. Buzzi *et al.*, Photomolecular High-Temperature Superconductivity, Phys. Rev. X **10**, 031028 (2020).
[73] M. Budden, T. Gebert, M. Buzzi, G. Jotzu, E. Wang, T. Matsuyama, G. Meier, Y. Laplace, D. Pontiroli, M. Riccò, F. Schlawin, D. Jaksch, and A. Cavalleri, Evidence for metastable photo-induced superconductivity in K_3C_{60}, arXiv:2002.12835.
[74] H. Gao, F. Schlawin, M. Buzzi, A. Cavalleri, and D. Jaksch, Photoinduced Electron Pairing in a Driven Cavity, Phys. Rev. Lett. **125**, 053602 (2020).